INTERNATIONAL JOURNAL OF ENERGY STUDIES

e-ISSN: 2717-7513 (ONLINE); homepage: https://dergipark.org.tr/en/pub/ijes

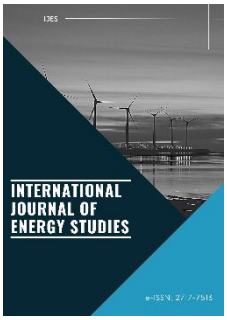

Research Article

Int J Energy Studies 2026; 11(1): 777-800

DOI: 10.58559/ijes.1822237

Received : 12 Nov 2025

Revised : 19 Feb 2026

Accepted : 13 Mar 2026

Evaluation of a CeO2 candidate material for nuclear experimental applications through thermal-hydraulic analysis with COBRA-TF in VVER-1200 reactor

Ahmet Kağan Mercan[a*], Fahrettin Eskiköy[b]

a Hacettepe University Nuclear Engineering Department, ORCID: 0000-0001-6263-5026

b Hacettepe University Nuclear Engineering Department, ORCID: 0009-0002-6202-065

*(*kaganmercan@hacettepe.edu.tr)*

Highlights

- CeO2 material properties are investigated to be able to utilized in tests and experiments instead of UO2.
- Research shows CeO2 has lower fuel temperatures in VVER-1200 nominal operation and transient conditions which allows performing experiments over UO2 melting limits.
- The higher thermal conductivity and lower specific heat capacity of CeO_2, together with its material characteristic similarity to UO_2, make it a suitable surrogate fuel material in nuclear fuel experiments. Its use enables experimental investigations under non-irradiated conditions and allows the creation of test systems operating at elevated temperature regimes without the safeguards associated with UO_2.

You can cite this article as: Mercan AK, Eskiköy F. Evaluation of a CeO2 candidate material for nuclear experimental applications through thermal-hydraulic analysis with COBRA-TF in VVER-1200 reactor. Int J Energy Studies 2026; 11(1): 777-800.

ABSTRACT

Uranium dioxide (UO_2) has long been used as the standard fuel in pressurized water reactors (PWRs) such as the VVER-1200. However, its radioactive nature, high fabrication cost, and regulatory constraints present significant challenges for experimental studies. In this work, cerium dioxide (CeO_2), a non-fissile and chemically stable ceramic, is investigated as a potential surrogate for UO_2 in thermal-hydraulic experiments. Using the COBRA-TF (CTF) subchannel analysis code, a VVER-1200 fuel assembly was modeled to simulate the thermal behavior of both UO_2 and CeO_2 under steady-state and transient conditions, including reactivity insertion and loss-of-flow accidents.

Simulation results indicate that CeO_2's lower thermal conductivity and specific heat capacity lead to higher fuel centerline temperatures—up to 200 °C higher during normal operation and approximately 120 °C during transient events. While these elevated temperatures reflect conservative predictions, the fuel surface and cladding temperatures remain comparable to UO_2, supporting CeO_2's suitability for experimental investigations such as cladding oxidation or material testing. Additionally, similar Critical Heat Flux Ratio (CHFR) values in both materials confirm CeO_2's applicability in replicating coolant thermal conditions. These findings suggest that CeO_2 can serve as a viable experimental substitute to study key fuel and cladding behaviors without the complexities of handling radioactive UO_2.

Keywords: CeO_2, VVER-1200, COBRA-TF, LOFA, RIA

1. INTRODUCTION

In pressurized water reactors (PWRs) such as the VVER-1200, uranium dioxide (UO_2) has long been the standard nuclear fuel. However, UO_2 is a radioactive material, poses challenges related to radiation hazards and handling safety, which complicates its use and management in nuclear applications. Therefore, extensive safety measures are required to control and prevent radiation emissions. Also, mining, fabrication and testing by using UO_2 fuel can be extremely expensive and many legal processes should be involved for nuclear security. Considering thermal-hydraulic experiments using fuel alternative can also lead to melting of the material and investigation of cladding like structures in high temperature environment, using cheaper and safer alternative will be beneficial for continous investigation and research. All activities involving the use of nuclear fuel fall under the scope of nuclear safeguards administered by the International Atomic Energy Agency (IAEA). Accordingly, experimental tests and research activities utilizing nuclear fuels are subject to rigorous regulatory controls and intensive oversight, including inspection, verification, and compliance mechanisms, in order to ensure adherence to international nuclear safety, security, and non-proliferation frameworks [1].

Alternatively, a rare earth element of Cerium Dioxide (CeO_2), also known as cerium(IV) oxide, is a chemically stable, non-fissile ceramic compound that has gained attention as a potential surrogate or alternative fuel material in nuclear thermal-hydraulic studies [2]. Detailed characterization of the CeO_2 analogue ceramics, detailed morphology, crystallography and chemistry are investigated to be able to use material is geological disposal together within spent nuclear fuel [3]. CeO_2 is a yellow-white powder and a common oxide of the rare earth element cerium, typically encountered as an intermediate during the purification of cerium from its ores. While its primary industrial applications include use as a high-precision glass polishing agent, with a density of 7215 kg/m^3, CeO_2 is notably less dense than UO_2, which may have implications for heat transfer characteristics and structural considerations [4]. Notably, its high melting point of approximately 2600°C makes it particularly attractive for high-temperature reactor applications [4], as it can withstand severe thermal conditions without undergoing phase changes or degradation. Although CeO_2 is not a fissile material and therefore cannot be used to generate nuclear energy through fission, this material can be utilized instead of UO_2 in experimental works to be able to represent characteristics of nuclear fuel under major pressure and temperature conditions. The key advantage of using surrogate material like CeO_2 instead of UO_2 is safer than using radioactive material and inexpensive compared to the traditional fuel rods.

COBRA-TF (Coolant Boiling in Rod Arrays – Two Fluid) is a subchannel thermal-hydraulic code actively utilized for investigating the thermal hydraulic behavior of nuclear fuel system during both normal operation and transients in Pressurized Water Reactors (PWRs) and Boiling Water Reactors (BWRs) [5]. The COBRA-TF (CTF) allows modelling of both pin-by-pin and assembly-by-assembly structures and is able to calculate how core thermal hydraulic parameters change during both steady-state and transient conditions. Different fuel, clad and structural models can be modelled on the code and temperatures of selected materials, heat transfer between structures, flow condition change can be evaluated. The code is well-validated for VVER based structures and actively used in worldwide. [6] [7]

In this study, thermal properties of CeO_2 material were investigated using CTF sub-channel accident code and its usability in experiments in the operating and accident scenario environment of the VVER-1200 reactor. After development of VVER-1200 assembly model on COBRA-TF, investigated thermal properties of CeO_2 is modelled on CTF and the results of both steady-state and accident conditions are compared. Performed simulations are conducted on average fuel channel to investigate key parameters such as fuel centerline and surface temperatures, cladding surface temperature, local heat flux, and departure from nucleate boiling ratio (DNBR).

2. METHODOLOGY

2.1. Investigation of Thermal Conductivity Models

The thermal conductivity equation developed by Harding and Martin for fully dense solid UO_2 is based on a detailed theoretical analysis and is applicable over the temperature range from 773 K up to the melting point at 3120 K [8]. This model was chosen due to its strong theoretical foundation, good agreement with earlier empirical correlations derived from experimental data, and consistency with in-reactor integral measurements up to the melting point. Although the recommended temperature range is 773–3120 K, the equation also aligns well with other models that fit the data at lower temperatures. Therefore, the Harding and Martin equation is considered the most reliable. representation of the thermal conductivity k (in $Wm^{-1}K^{-1}$) for fully dense UO_2 within the specified temperature range. The equations for thermal conductivity are expressed in $Wm^{-1}K^{-1}$ is given below where T is temperature in K and k_b is the Boltzmann constant $8.6144 \times 10^{-5} eVK^{-1}$.

$$k_{UO2}^{Harding}(T) = \frac{1}{0.0375+2.165\times10^{-4}\times T} + \left(\frac{4.715\times10^{9}}{T^2}\right) \times \exp\left(\frac{-16361}{T}\right) \quad (1)$$

$$k_{UO2}^{Brandt}(T) = \frac{1}{0.0439+2.16\times10^{-4}\times T} + 0.112 \times T \times \exp\left(\frac{-1.18}{k_b\times T}\right) - 4.18 \times 10^{5} \times \exp\left(\frac{-3.29}{k_b\times T}\right) \quad (2)$$

The first term represents the phonon contribution. The second term accounts for electronic conduction, while the third term describes the decrease in conduction attributed to dislocations at high temperatures. [9]

This study uses the thermal conductivity of stoichiometric CeO_2. This was achieved by measuring thermal expansion (from 313 to 1723 K), thermal diffusivity (from 298 to 1473 K), and specific heat capacity (from 313 to 1373 K). The thermal conductivity was subsequently calculated as the product of the measured density, thermal diffusivity, and specific heat capacity [10]. The equation 3 is given below for calculation of thermal conductivity of CeO_2.

$$k_{CeO_2}(T) = \frac{1}{A+B\times T} \quad (3)\ [10]$$

where A= 6.776×10^{-2} m·K·W^{-1} and B= 2.793×10^{-4} m·W^{-1} Thermal conductivity values of UO_2 with both two equation and CeO_2 is W/m-K.

Figure 1 presents thermal conductivity value change of UO2 and thermal conductivity values for CeO2 for input of CTF simulation [10]. CeO_2 exhibits lower thermal conductivity than UO_2 across all temperature ranges, starting from 5.82 W/m-K compared to UO_2's W/m-K at room temperature and decreasing to 1.97 W/m-K and 2.64 W/m-K respectively at 1589 K, with this difference narrowing at higher temperatures. As seen, the use of CeO_2 will probably result in higher temperatures being obtained in experiments due to its higher conductivity value, but this may provide more conservative results in the calculations and evaluation of safe operating limits of Critical Heat Flux Ratio of 1.3 for pressurized light water reactor, fuel and cladding melting temperature which are 2600℃ and 1200℃ respectively, stress and strain of the fuel in the experiments performed.

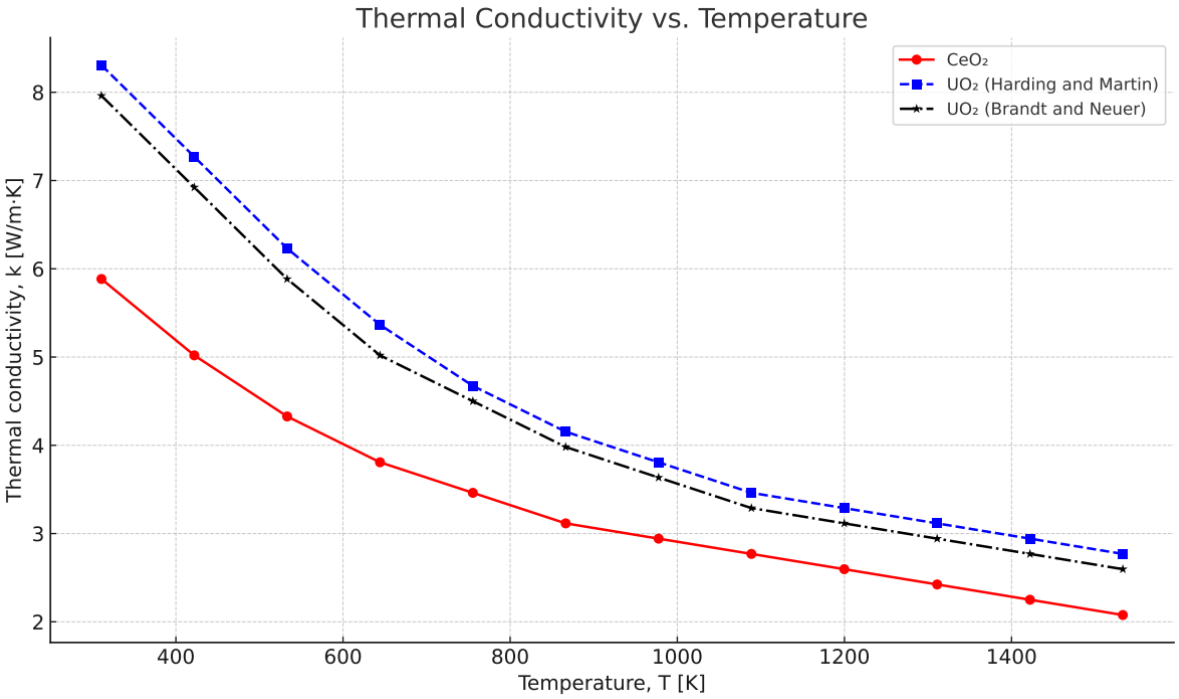

Figure 1: The calculated temperature dependant conductivity values of UO2 and CeO2

2.2. Investigation of Specific Heat Capacity

The specific heat capacity of solid UO_2 was modelled using the equation recommended by Fink et al., which is based on an extensive assessment of experimental data over the temperature range of 298.15 K and 3120K. For solid UO_2, its heat capacity is reliably derived as the temperature derivative of its enthalpy increment equations, as other thermodynamic contributions to heat capacity are considered negligible. The equations established by Fink et al. for the heat capacity of UO_2 are then detailed below.

$$c_p(T) = \left(\frac{C_1 \theta^2 \exp\left(\frac{\theta}{T}\right)}{T^2 \left(\exp\left(\frac{\theta}{T}\right) - 1\right)^2} + 2C_2 T + C_3 k_b \exp\left(\frac{-E_a}{k_b T}\right)\left(1 + \frac{E_a}{k_b T}\right) \right) \frac{100}{27 \times 4184} \quad (4)\ [9]$$

where

$\theta = 516.12$ K,

$C_1 = 78.215$ J·mol^{-1}·K^{-1},

$C_2 = 3.8609 \times 10^{-3}$ J·mol^{-1}·K^{-2},

$C_3 = 3.4250 \times 10^{8}$ J·mol^{-1}·eV^{-1},

$E_a = 1.9105$ eV,

$k_b = 8.6144 \times 10^{-5}$ eV·K^{-1},is the Boltzmann constant [9],

In this study, the specific heat capacity values of CeO_2 were obtained from the thermophysical property data reported by Nelson et al. (2014) [10]. The data were incorporated into the COBRA-TF simulation environment to accurately model the thermal response of CeO_2 under conditions representative of reactor operation. Leveraging this experimentally evaluated dataset enabled a reliable comparison between CeO_2 and UO_2 with regard to temperature distribution, heat removal efficiency, and overall thermal performance.

Table 1: The specific heat data of CeO2 taken from **[9]**

Temperature(K)	**Specific Heat (J/kg-K)**
211	386.41
391	405.12
571	425.20
751	435.43
931	437.19
1111	442.23
1291	448.76
1471	456.99
1651	461.76
2011	469.94
2371	479.97

Conversely to the conductivity, **Figure 2** shows that CeO_2 demonstrates significantly higher specific heat capacity, starting from 385.18 J/kg·K compared to UO_2's 259.58 J/kg·K at room temperature and increasing to 481.48 J/kg·K and 334.94 J/kg·K respectively at 1584.3 K. These results, together with the conductivity data, may cause the fuel centerline temperature to be higher than expected.

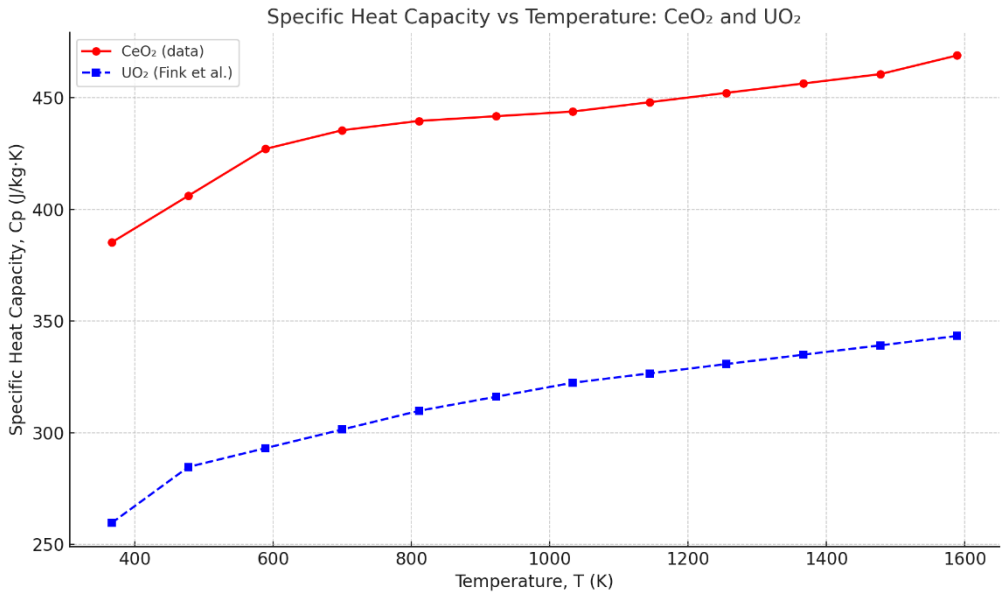

Figure 2: The comparison of specific heat capacity of UO_2 and CeO_2

3. VVER-1200 CORE CTF MODEL

In this study, an assembly channel of VVER-1200 is modelled on CTF code to calculate temperature distribution of the fuel structures as well as clad temperature. The core structure of the VVER-1200 type reactor, which is under construction in various countries, is similar to previous designs [11].

The plant overview of VVER-1200 is shared in **Table 2**. The CTF model data used for modelling of VVER-1200 is given in **Table 3**. The implemented power profile is given in **Figure 3**. The relative power is defined to the each node to be able represent reactor power distribution as boundary condition.

Table 2: The plant overview of VVER-1200 [12]

Parameter	**Value**
Net Electrical Output	1200 MWe
Thermal Power Rating	3200 MWt
Gross Electrical Output	~1250 MWe (depends on turbine-generator configuration)
Plant Thermal Efficiency	~34.8–35.9 %%

Number Of Power Generation Units	Up to 12
Nominal Plant Capacity Factor	≥ 90%
Total Plant Protected Area	~80 acres (varies by site)
Total Owner-Controlled Area	~200–250 acres (varies by site)
Steam Generator Number	Four horizontal steam generators
Steam Generator Type	Horizontal tube-and-shell type
Steam Cycle	Superheated steam, saturated cycle with moisture separator-reheater
Turbine Throttle Conditions	~6.0 MPa & ~270°C (varies by turbine supplier)
Steam Flow	~4800 t/h
Feedwater Temperature	~220°C
Saturation Temperature	~275–280°C
Operating Pressure	15.7 MPa
Fuel Type	UO_2
Fuel Design	18x18 or 17x17 lattice ~312 fuel assemblies
Fuel Cladding	Zirconium alloy (Zr+Nb)
Refueling Interval	18 months (with flexible core design allowing extended cycles)

Table 3: The VVER-1200 core specification used in CTF

Parameter	Value	Parameter	Value
Fuel Pellet Diameter(mm) [13]	7.6	Initial Operating Pressure (MPa)	16.2 [14]
Rod diameter(mm) [13]	9.1	Inlet Coolant Temperature(K)	594 [14]
Clad thickness(mm) [13]	0.685	Inlet Enthalpy (MJ/kg)	1327
Rod Pitch(mm) [13]	12.75	Total Coolant mass flow rate(kg/s)	23889 [14]
Central Hole Diameter (mm)	0.25	Average linear heat generation rate(kW/m)	16.78 [14]
Number of fuel assemblies in core [13]	163	Constant gap conductance($kW/m^2 \cdot K$)	28400
Number of fuel rod per fuel assembly [13]	312	Channel Length(m)	4.0767
Number of Total rods	50856	Fuel Density	10.78 g/cm^3[taken from [15]]

Primarily, the temperature distribution in fuel, cladding and coolant is compared in nominal reactor condition at steady conditions. This will help identifying potential differences on time-depended transient calculations. The time-depended calculations for reactivity insertion and loss-of-flow conditions are employed to investigate behaviour during transient conditions.

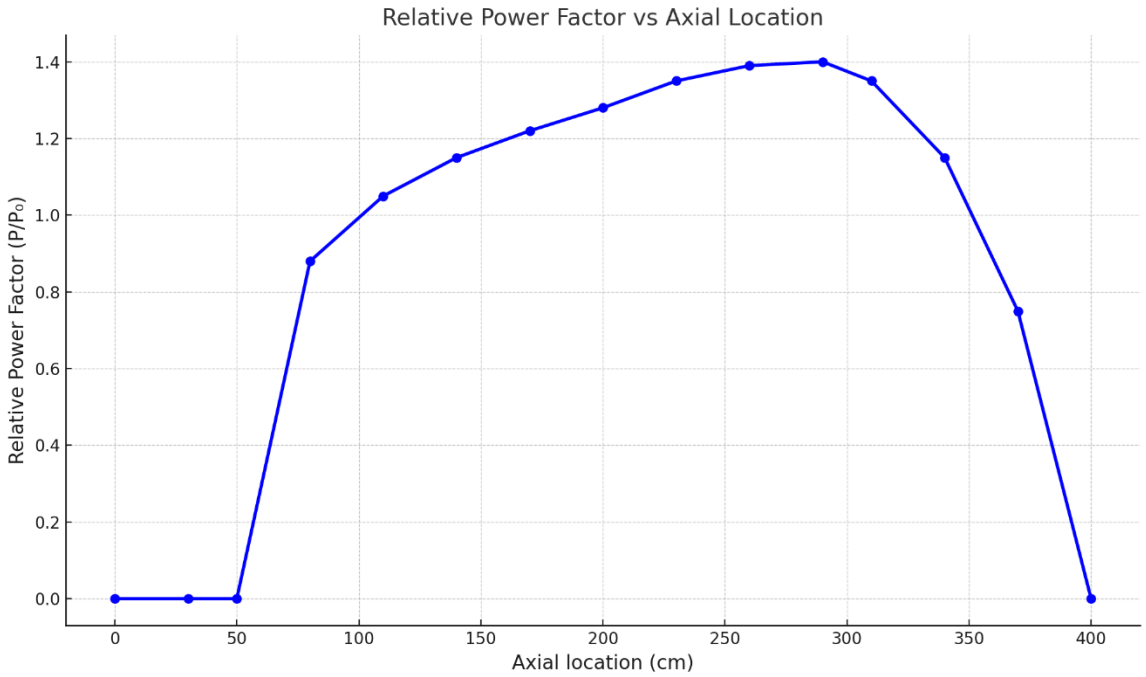

Figure 3: The employed power distribution over vertical location for VVER-1200 reactor core modified from **[16]**

To be able to investigate the behaviour during a hypothetical accident scenario, the reactivity insertion accident (RIA) as well as loss of flow accident (LOFA) cases are investigated. The following point-kinetics equations is solved for 20$ of reactivity insertion which is the highest worth for control rods [17] and time depended power response of the core is given in **Figure 4**.

$$\frac{dn(t)}{dt} = \frac{\rho(t)-\beta}{\Lambda} n(t) + \sum_{i=6}^{6} \lambda_i C_i(t) + S(t) \quad (5)\ [18]$$

$$\frac{dC_i(t)}{dt} = \frac{\beta_i}{\Lambda} n(t) - \lambda_i C_i(t) \quad (6)\ [18]$$

Where n is atom number, ρ is reactivity in pcm , β is delayed neutron fractions, Λ generation time in μs, C is number of delayed neutrons and λ is decay rate of delayed neutrons in 1/s.

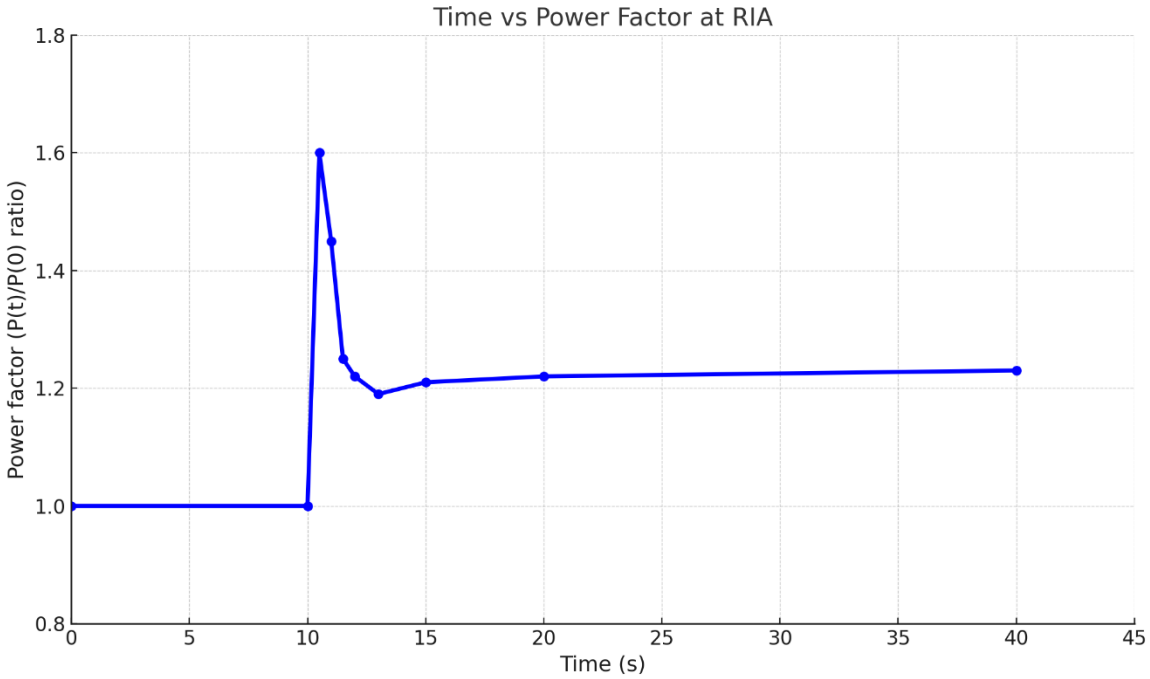

Figure 4: Time depended power response of the core for 20$ of reactivity insertion

For the assessment of potential impact of LOFA case, the flow rate is decreased to 75% on its nominal value and 25% of its nominal value, respectively.

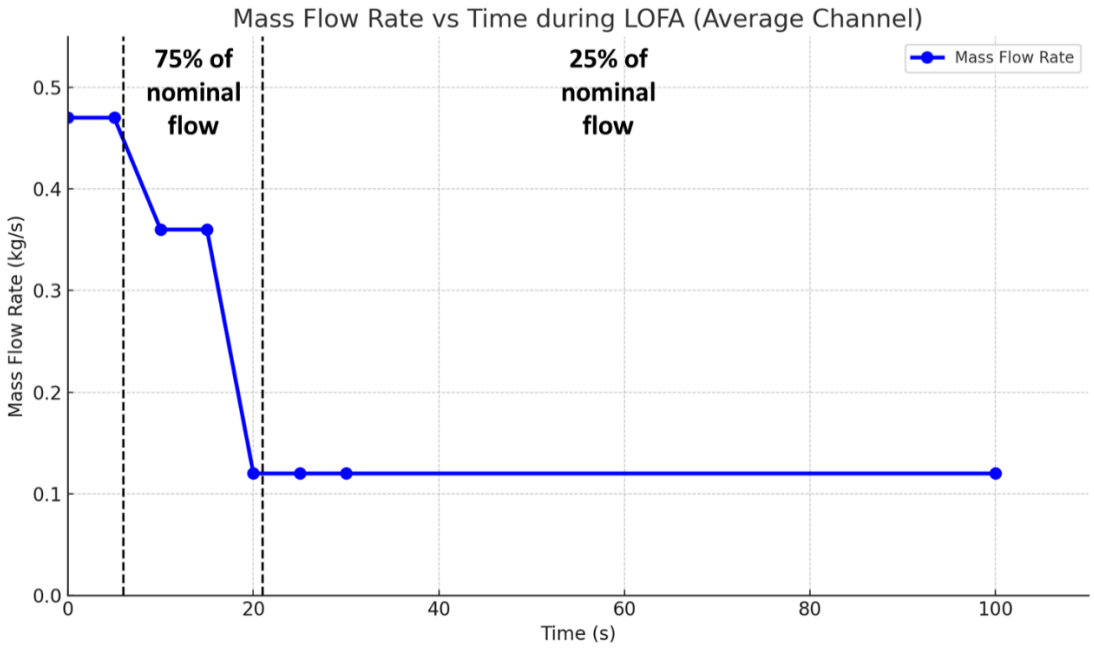

Figure 5: The flow rate change in time to model LOFA case

Finally, the nonuniform model of minimum heat flux model is used for evaluating Critical Heat Flux (CHF) and Critical Heat Flux Ratio (CHFR) [19]

4. THE DISCUSSION OF THE CTF SIMULATION RESULTS OF VVER-1200 WITH UO_2 AND CEO_2 MATERİALS

4.1. The Comparison of UO_2 and CeO_2 Materials in Nominal Operation Conditions

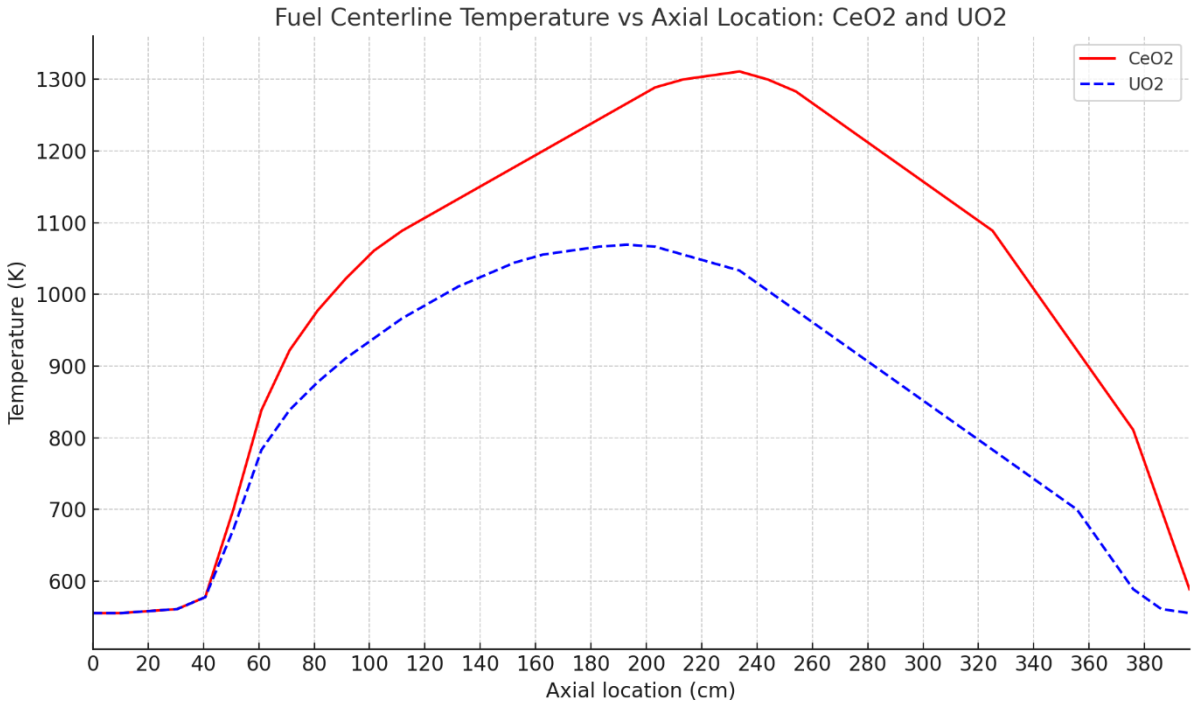

Figure 6: The comparison of calculated fuel centerline temperature for both UO_2 and CeO_2 by using CTF

Figure 6 illustrates the axial temperature change for given power information for investigated materials. As expected, higher specific heat capacity and lower conductivity of the CeO_2 results with higher fuel centerline temperature results. The highest temperature difference is about 250K. CeO_2's approximately 40-50% higher specific heat capacity would provide high thermal inertia during transient conditions due to storing large amounts of heat without changing the temperature drastically. [20]

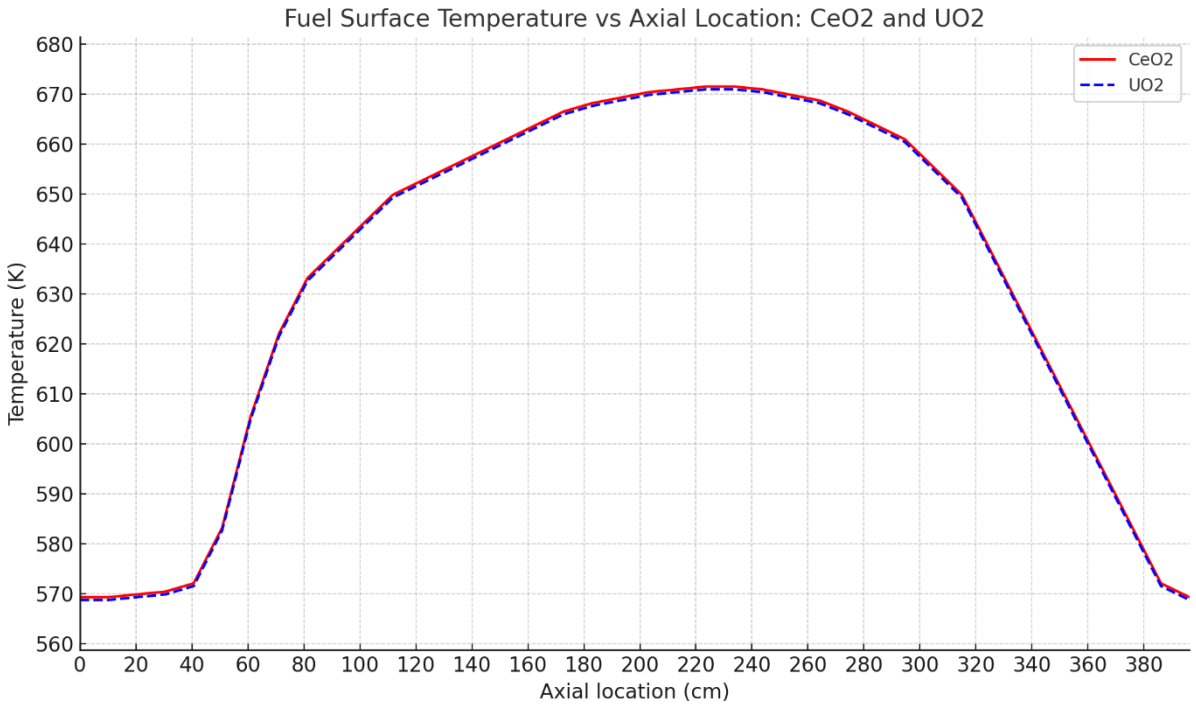

Figure 7: The comparison of calculated fuel surface temperature for both by using CTF

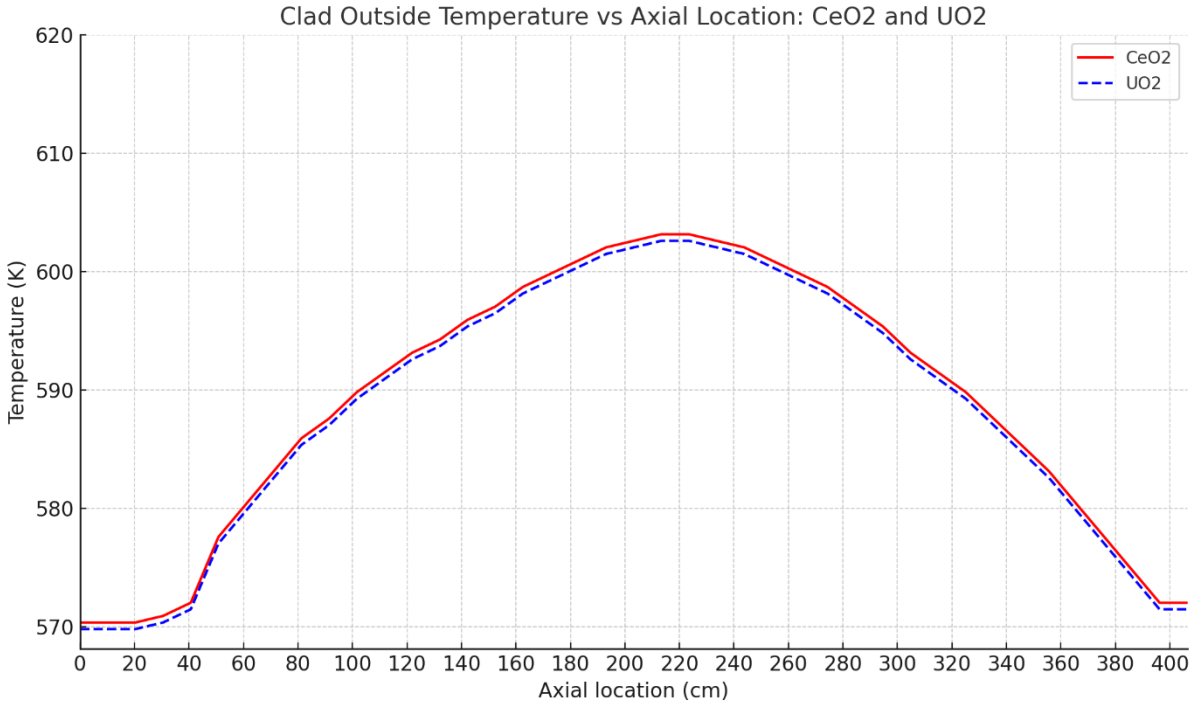

Figure 8: The comparison of calculated clad outside temperature for both by using CTF

The **Figure 7** and **Figure 8** show the comparison of the nominal operation temperatures of fuel surface and clad outside for two selected materials. Even though higher temperatures are obtained

in calculation of fuel centerline temperature, this difference is not visible on the results of fuel surface and clad outside temperatures. Since CTF calculates from starting fuel itself, the impact of fuel change represents itself in smaller order compared to the fuel. It can be stated that CeO_2 can be useful candidate for testing new cladding materials in reactor operation conditions.

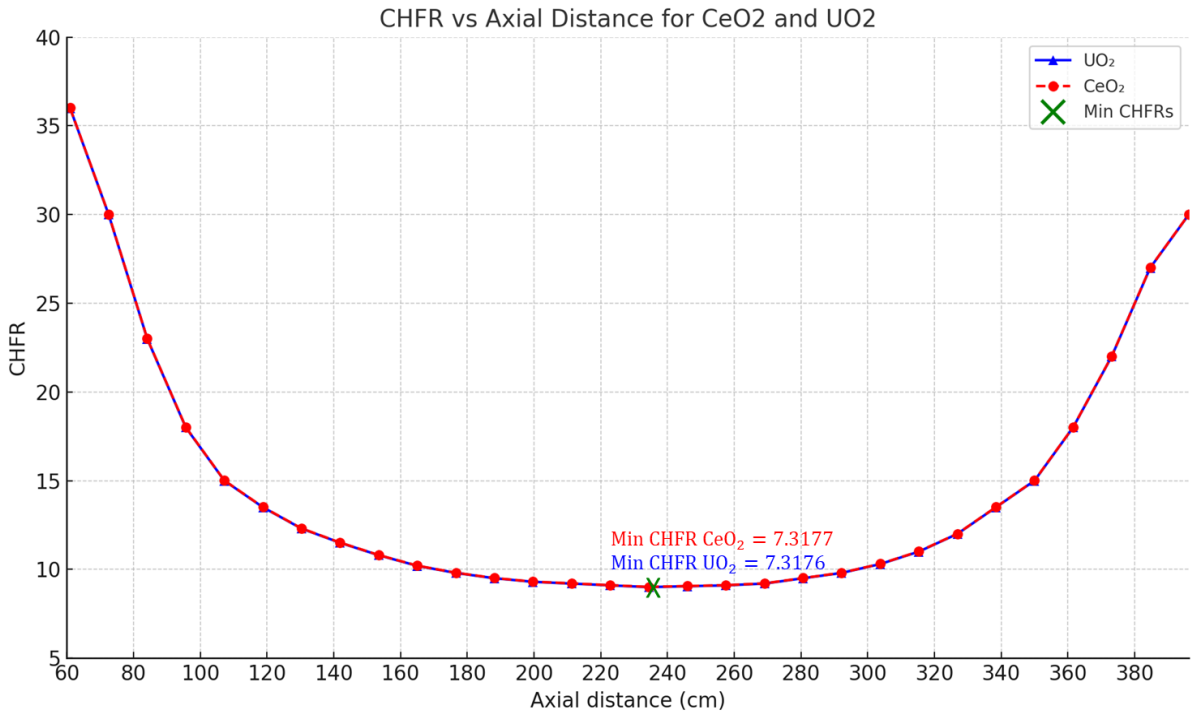

Figure 9: The comparison of calculated Critical Heat Flux Ratio (CHFR) values for both UO_2 and CeO_2 using CTF

Lastly, the critical heat flux ratio change along with the axial distance is given in **Figure 9**. The minimum value of CHFR is 7.3176 for UO_2 whereas this value is 7.3177 in case of CeO_2 is used. It indicates that this material can be used for evaluation of the safe operation limits during both normal operation and transient cases. CHF parameter is a function of mass flow rate and thermodynamic parameters of the coolant as well as heat flux, therefore, it is expected that CHFR change would be minimal since CTF calculation starts from the fuel.

4.2. The Comparison of UO_2 and CeO_2 Materials in RIA Conditions

After the initiation of the reactivity insertion, the maximum fuel centerline temperature change is shown in **Figure 10**. UO_2 is able to capture the power change trend in transient whereas CeO_2 temperature profile cannot capture decreasing trend after the initiation of reactivity. The main reason of the difference on the trend can be difference between thermal properties of CeO_2 and

UO_2. Higher specific heat and lower conductivity of CeO_2 reaches higher temperatures during steady-state part of the transient and it might result with the increase of temperature difference of used parameters during immense power rise due the reactivity.

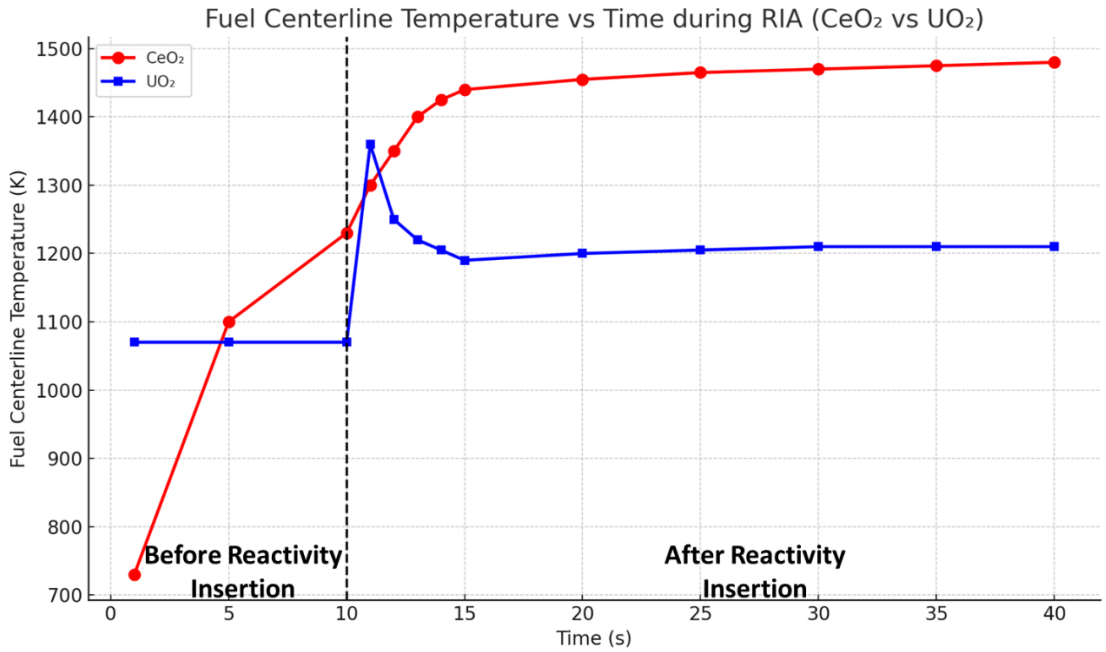

Figure 10: The calculated maximum fuel centerline temperature change due to reactivity insertion and feedback in time for both materials

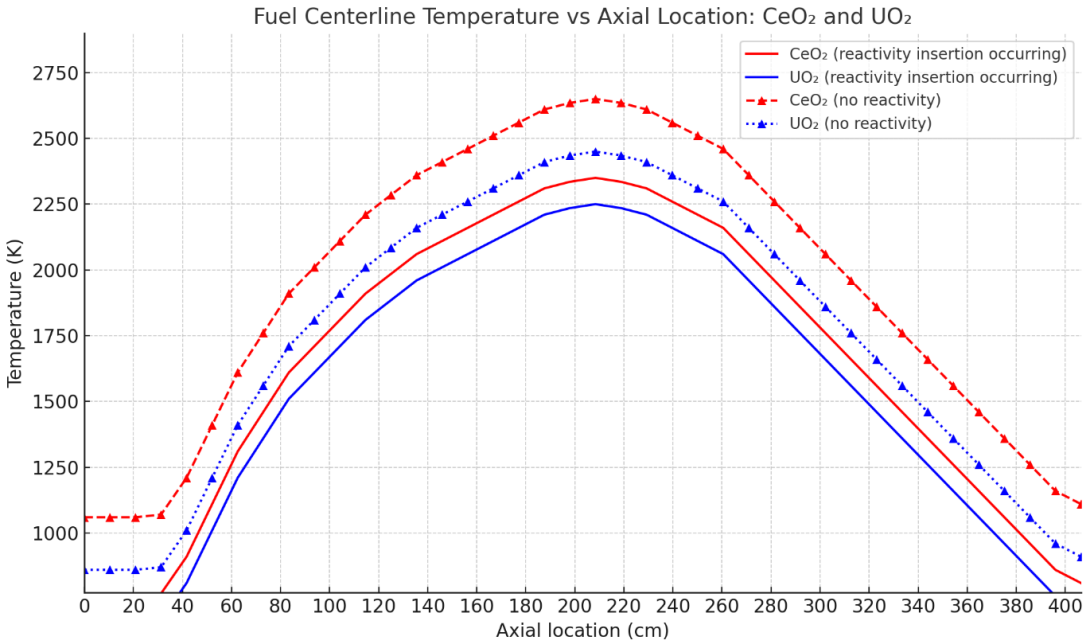

Figure 11: The comparison of calculated fuel centerline temperature change during RIA at the end of simulation for both UO_2 and CeO_2 using CTF

Figure 11 demonstrates the fuel centerline temperature change due to power response to the 20$ reactivity insertion for both CeO_2 and UO_2 fuels. Despite having same trend in both cases, CeO_2 has significantly higher temperature rise during the transient. The temperature of the centerline rises approximately 300 ℃ when CeO_2 is used, yet, UO_2 fuel centerline temperature increase is only about 200 ℃. Since CeO_2 has lower conductivity and higher specific heat leads to higher temperature rise during RIA. Hence, the results indicate that the transients in high temperatures might be more conservative than the one with UO_2 which might create margin when data is used in real life.

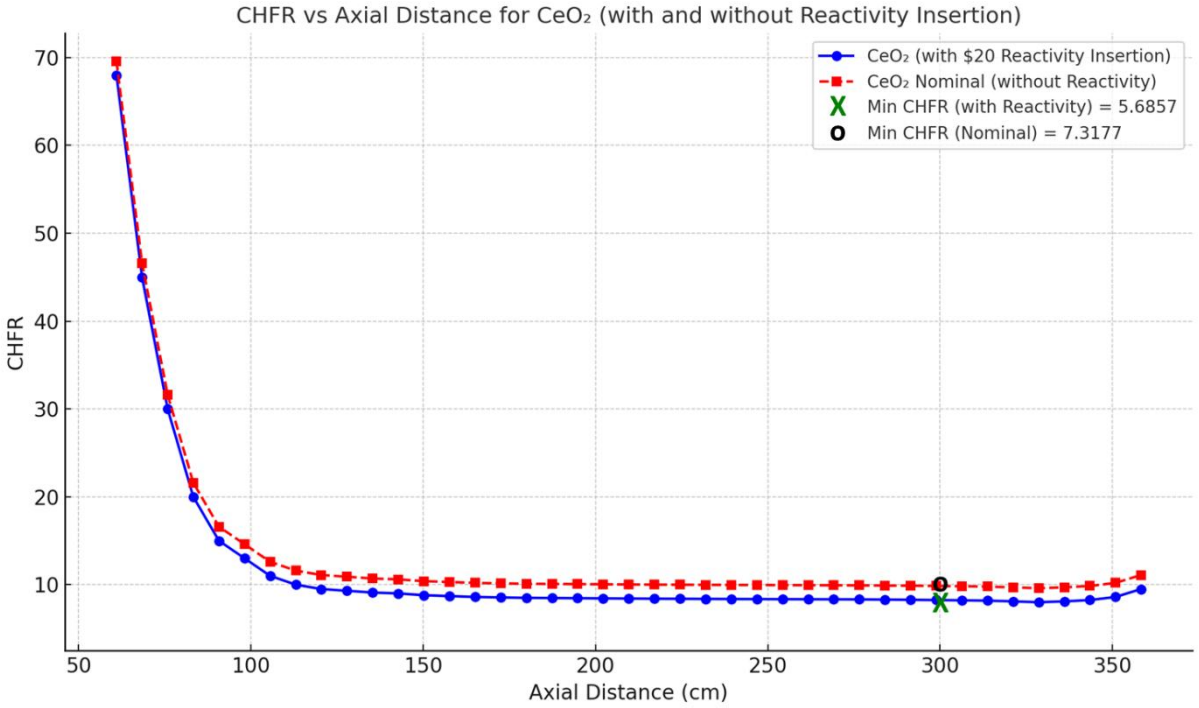

Figure 12: The calculated CHFR values during RIA transient at the end of simulation with CeO_2

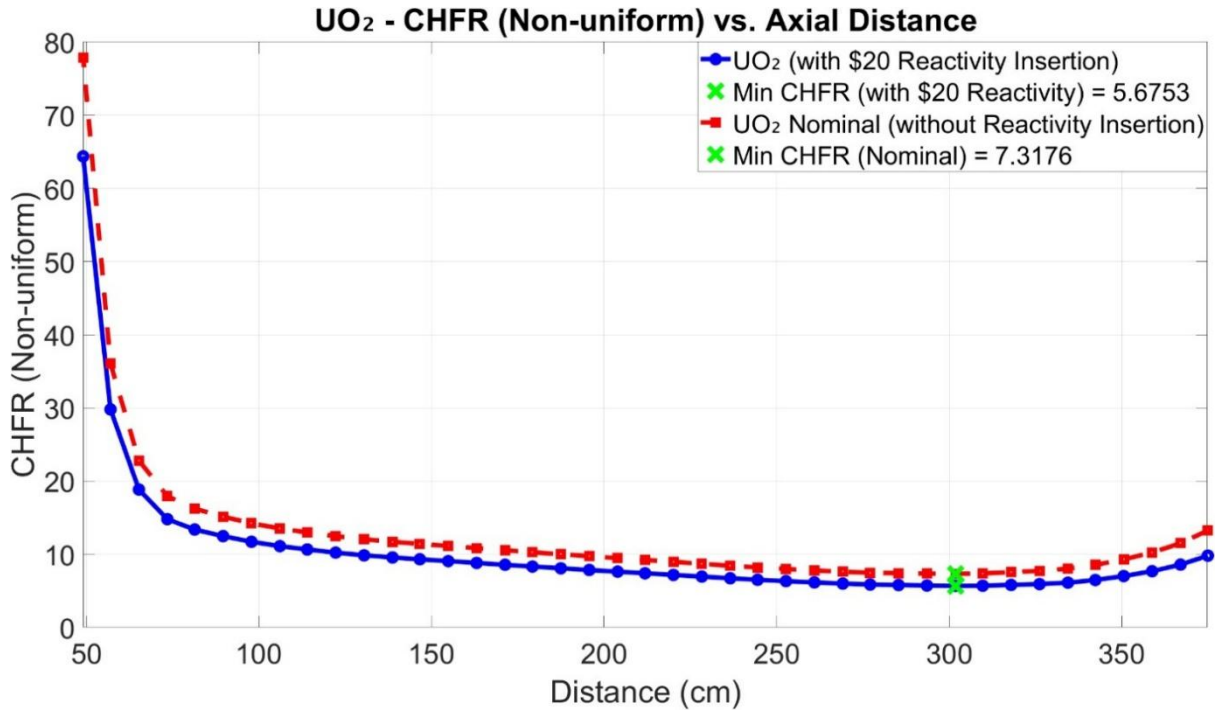

Figure 13: The calculated CHFR values during RIA transient at the end of simulation with UO_2

Figure 12 and **Figure 13** show CHFR change along with the rod axial distance during RIA transient for CeO_2 and UO_2, respectively. As expected, RIA profile can be captured in both cases. Similar, minimum CHFR values are obtained for both fuels, slightly lower in UO_2 case, which can indicate usability for estimating on safe operation condition. However, slightly lower values of CeO_2 might require additional attention in limiting cases of operation.

4.3. The Comparison of UO_2 and CeO_2 Materials in LOFA Conditions

For the LOFA transient, the flow is decreased 25% and 75% of its normal value to assess temperature change of fuel structure which corresponds to loss of one and three main coolant pump during operation, respectively. The maximum fuel centerline temperature change in time is shown in **Figure 14**. As expected, the maximum temperature increases due to loss of flow, however, CeO_2 temperature rises significantly larger than the one with UO_2. The main reason of this 200 K difference occurs from lower conductivity and higher specific heat of CeO_2. Hence, it should be noted that thermal response of experimental CeO_2 can be stronger than the one with UO_2 which might reach melting temperatures early but create margin when developing related safety approaches. Since CTF uses embedded UO_2 libraries, the calculation with UO_2 and consequently results fluctuate until the steady-state case is achieved. However, the results are more stable when external library is implemented like CeO_2 case.

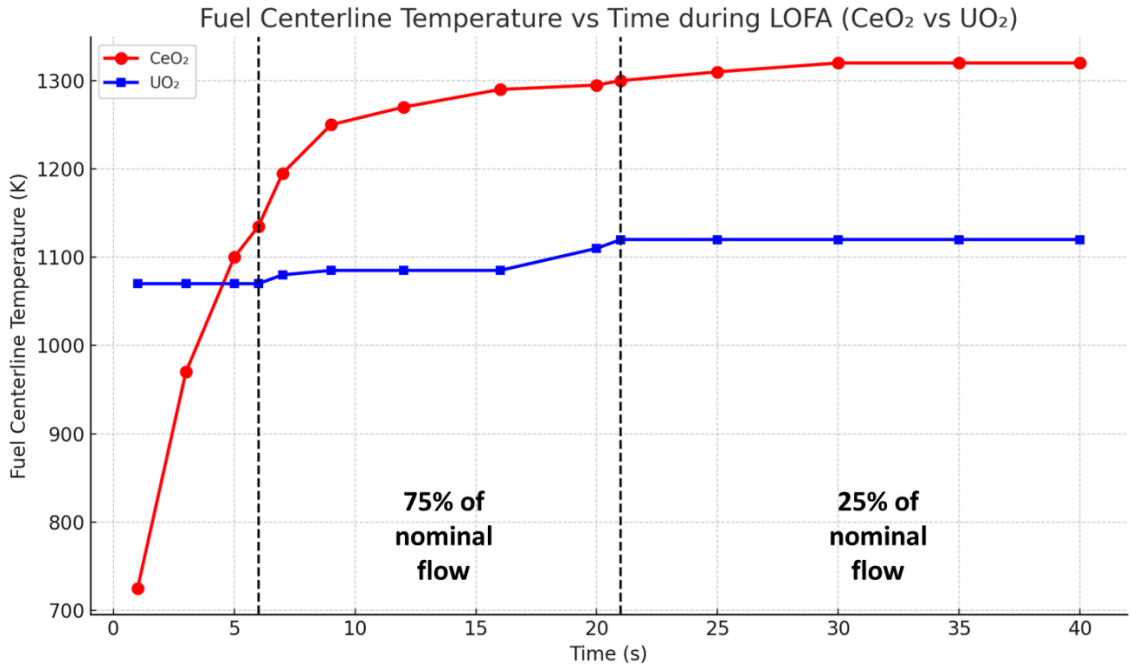

Figure 14: The calculated maximum fuel centerline temperature change due to loss of flow accident in time for both materials

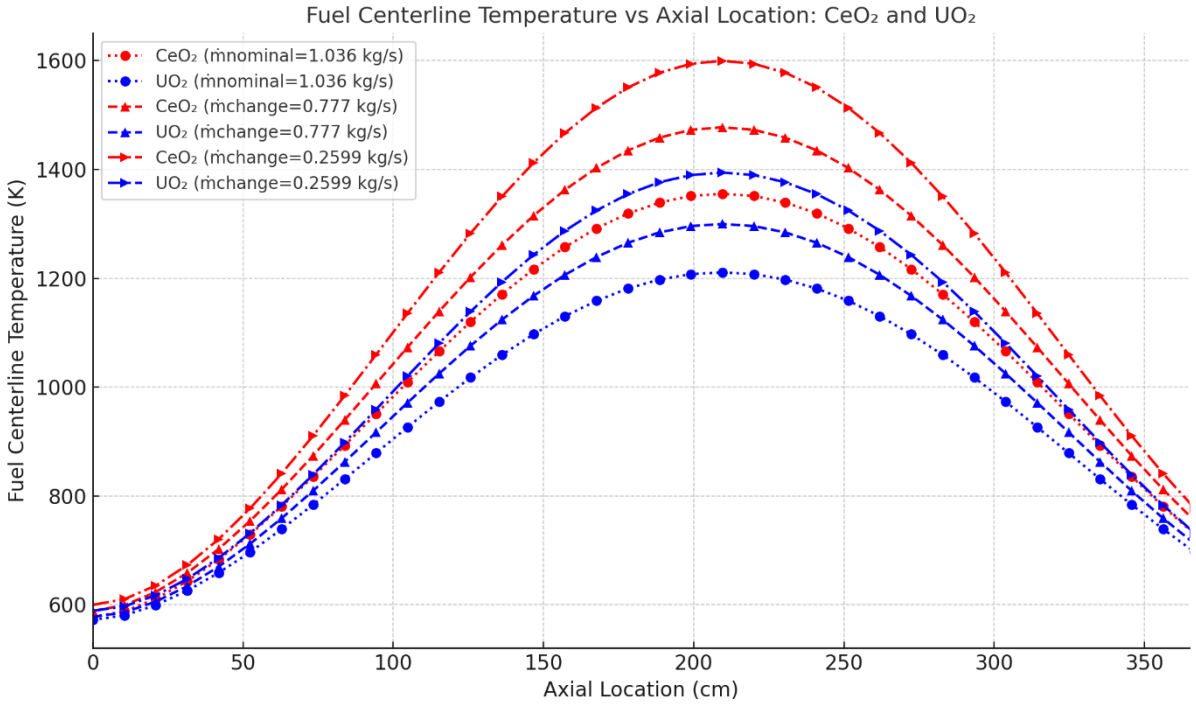

Figure 15: The comparison of calculated fuel centerline temperature at the end of simulation during LOFA case for both UO_2 and CeO_2 using CTF

The loss of flow accident as expected results with higher fuel centerline temperatures which can be seen in **Figure 15**. The CeO_2 case results with increase of the temperature to the about 1450K

and to the 1600K, respectively, when the flow decreases 25% and 75% of its normal value. This rise is significantly lower in the one with UO_2. It is direct result of thermal properties of CeO_2

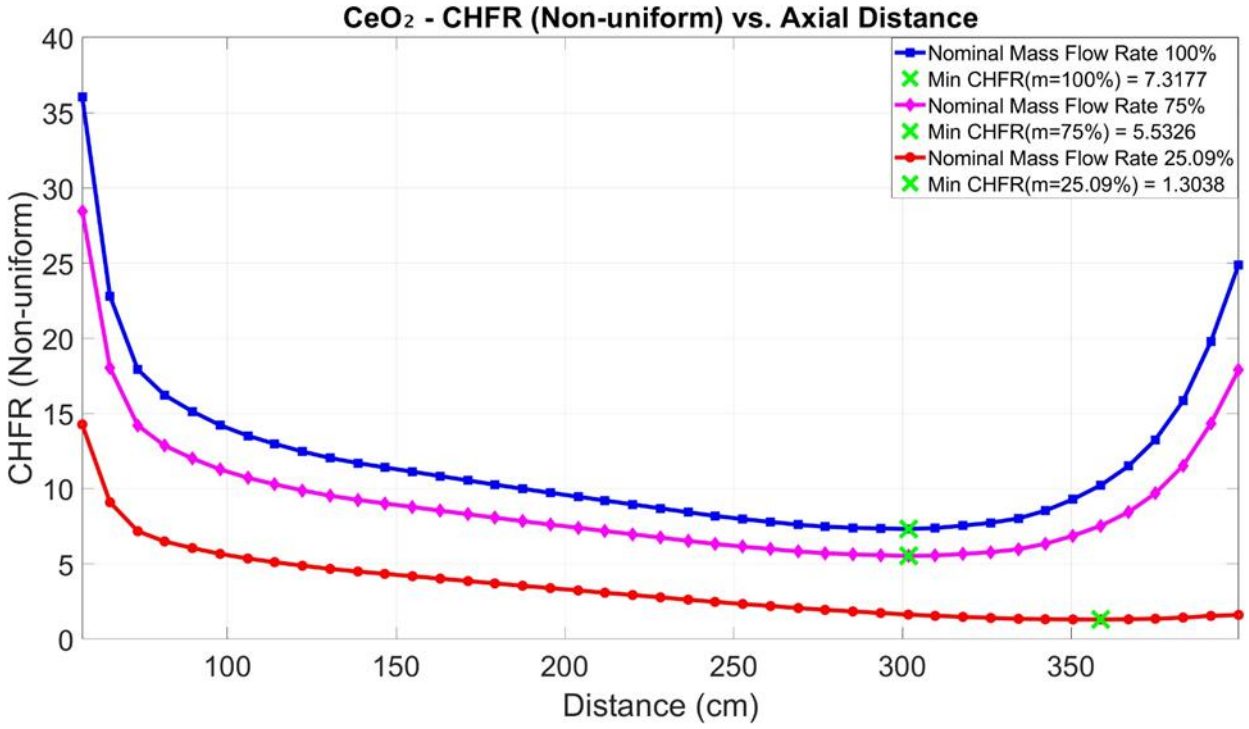

Figure 16: The calculated axial change of CHFR ratio at the end of simulation during LOFA case for CeO_2

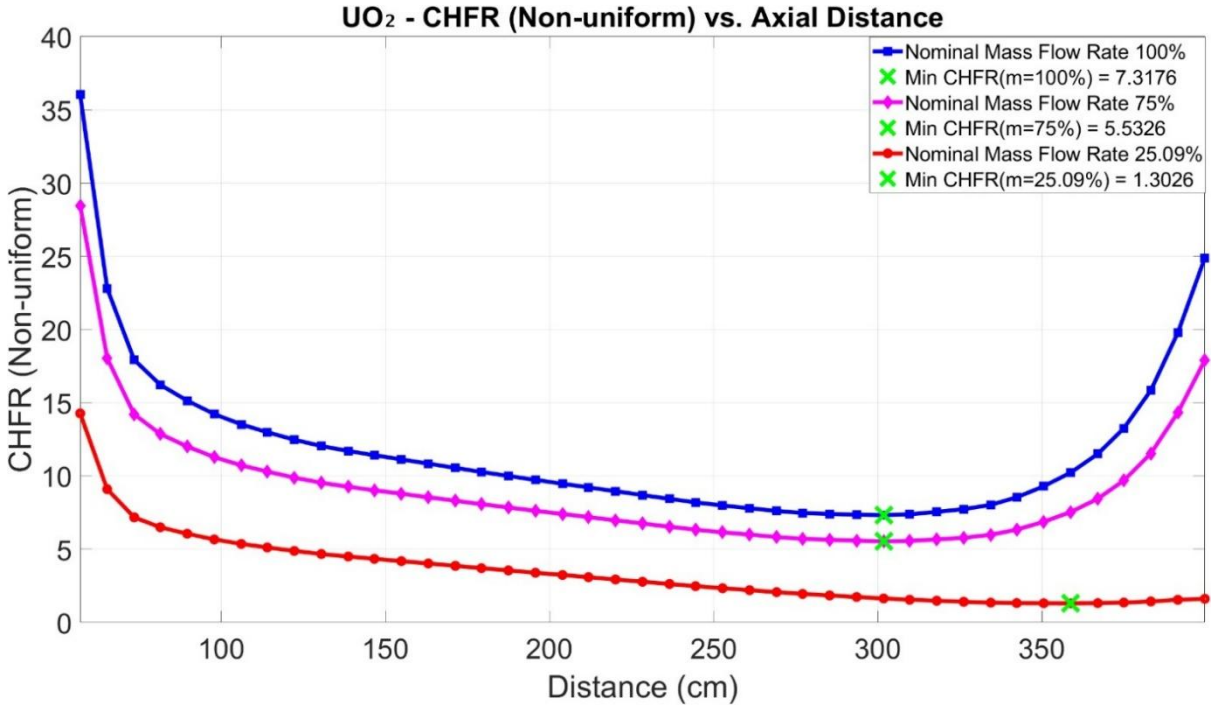

Figure 17: The calculated axial change of CHFR ratio at the end of simulation during LOFA case for UO_2

Figure 16 and **Figure 17** demonstrate the axial change of CHFR in loss-of-flow accident for CeO_2 and UO_2, respectively. It is evident that both materials show similar trend for same LOFA case. Indeed, safe operation limit of 1.30 is achieved when the main coolant flow decreases up to 25% of its original value for both fuel case. This situation indicates that material testing such as newer cladding, coated clads can be performed by using CeO_2 and results would be conservative and safer compared to the UO_2.

5. CONCLUSION

In this work, CeO_2 ceramic material thermal properties are investigated and compared with traditional fuel of UO_2 to be able to use in experimental environment to avoid extreme UO_2 fuel costs, to overcome potential nuclear security issues arising from the procurement of nuclear fuel to be used in experiments and radiation safety. The thermal properties of both CeO_2 and UO_2 are used in VVER-1200 reactor environment to investigate fuel thermal behaviour during both normal operation and transients by using CTF subchannel analysis code.

After the investigation performed on both materials using CTF in VVER-1200 geometry, following outcomes can be reached:

- Lower thermal conductivity and higher specific heat capacity of CeO_2 might result in obtaining higher fuel centerline temperatures. This situation might help to conservative approach on evaluating experimental results. However, experimental evaluation for thermal properties of CeO_2 can further upgrade the results.
- In VVER-1200 normal operation conditions, the temperature difference on both materials can reach up to 478 K. As mentioned before, thermal property difference shows itself in the calculations. Yet, the difference on temperature of fuel surface and clad outside is almost similar which shows CeO_2 can be utilized in certain experiments like testing new cladding materials or oxidation. Similar approach is used in experiments such as QUENCH [21] [22].
- The 20$ reactivity insertion and following power response results in similar responses on the fuel, yet, CeO_2 fuel centerline temperature rise is approximately 390 K higher than the one with UO_2. Considering that these materials have similar fuel melting temperatures, more conservative and rapid results can be obtained in experiments in RIA cases.
- Similar fuel behaviour is observed during RIA and LOFA cases. The CeO_2 material might be utilized to investigate clad behaviour, gap heat transfer change due to burn-up, chemical

and physical processes seen during severe accident conditions such as oxidation, breakaway phenomena or reflooding without damaging expensive UO_2 fuels.

- Almost the same CHFR values are obtained in both normal operation and accident cases indicating this material can also be used for predicting coolant conditions during both nominal and hypothetical accident conditions.

The main conclusion drawn from the analyses indicates that CeO_2 can replicate the thermal profile of UO_2 in certain experimental studies and research applications. This correspondence is observed under both steady-state conditions and selected transient scenarios. Therefore, CeO_2 may be utilized as a substitute for UO_2 in experiments that would otherwise require costly handling procedures, radioactive material management, and compliance with strict nuclear regulatory standards. Furthermore, since the thermophysical properties of CeO_2 tend to result in higher temperature predictions compared to UO_2, the outcomes of such studies may be inherently more conservative. This characteristic aligns well with the principles of nuclear safety culture.

In future, assembly by assembly model of CTF will be generated for VVER-1200 reactor core to simulate thermal-hydraulic behaviour of the subchannel realistically. Also, TRANURANUS model will be coupled with CTF to represent fuel properties in accurate manner, especially required for rapid transients. TRANSURANUS calculates material behaviour such as impact of cracking of fuel and thermophysical property change under irradiation which can enlighten potential difference between CeO_2 and UO_2 in high burnup conditions [23].

NOMENCLATURE

PWR – Pressurized Water Reactors

IAEA – International Atomic Energy Agency

COBRA-TF - Coolant Boiling in Rod Arrays – Two Fluid

CTF – COBRA-TF

DNBR – Departure from Nucleate Boiling

RIA – Reactivity Insertion Accident

LOFA – Loss of Flow Accident

CHFR- Critical Heat Flux Ratio

ACKNOWLEDGMENT

The authors express their gratitude to the Hacettepe University Nuclear Engineering Department for allowing them to use its infrastructure.

DECLARATION OF ETHICAL STANDARDS

The authors of the paper submitted declare that nothing which is necessary for achieving the paper requires ethical committee and/or legal-special permissions.

CONTRIBUTION OF THE AUTHORS

Ahmet Kağan Mercan: Supervision, Writing and editing of manuscript, development of methodology, performed analysis

Fahrettin Eskiköy: Writing and editing of manuscript, visualization of results, performed analysis

CONFLICT OF INTEREST

There is no conflict of interest in this study.

REFERENCES

[1] IAEA. IAEA Safeguards Serving Nuclear Non-Proliferation, IAEA Department of Safeguards, Vienna, 2012.

[2] Suzuki K, Kato M, Sunaoshi T, Uno H, Carvajal-Nunez U, Nelson AT, McClellan KJ. Thermal and mechanical properties of CeO2, Journal of the American Ceramic Society, cilt 102, 2018.

[3] Stennett MC, Corkhill CL, Marshall LA, Hyatt NC. Preparation, characterisation and dissolution of a CeO2 analogue for UO2 nuclear fuel, Journal of Nuclear Materials, cilt Volume 432, no. Issues 1–3, pp. Pages 182-188, 2013.

[4] Kurt J Lesker Company. Cerium Oxide CeO2 Evaporation Process Notes, [Çevrimiçi]. Available:https://www.lesker.com/newweb/deposition_materials/deposition-materials-notes.cfm?pgid=ce2#. [Erişildi: 4 July 2025].

[5] US NRC. COBRA/TRAC- A Thermal-Hydraulics Code for Transient Analysis of Nuclear Reactor Vessels and Primary Coolant Systems, U.S. NRC, 1983.

[6] Zhao X, Wysocki A, Shirvan K, Salko R. Assessment of the Subchannel Code CTF for Single- and Two-Phase Flows, Nuclear Technology, cilt 205, pp. 338-351, 2019.

[7] Toth I. The VVER Code Validation Matrix and VVER Specificities, Seminar on the transfer of competence, knowledge and experience gained through CSNI activities in the field of thermal-hydraulics(THICKET2008), Pisa, Italy, 2008.

[8] Harding J, Marting D. A recommendation for the thermal conductivity of UO2, Journal of Nuclear Materials, pp. 223-226, 1989.

[9] Fink JK, Petri MC. Thermophysical Properties of Uranium Dioxide, Argonne National Laboratory, Argonne, IL, USA, ANL/RE-97/2, Feb. 1997.

[10] Nelson AT, Rittman DR, White JT, Dunwoody JT, Kato M, McClellan KJ. An Evaluation of the Thermophysical Properties of Stoichiometric CeO2 in Comparison to UO2 and PuO2, Journal of the American Ceramic Society Journal of the American Ceramic Society, vol. 97, no. 11, 2014, Available: https://ceramics.onlinelibrary.wiley.com/doi/10.1111/jace.13170. [Accessed 4 July 2025].

[11] Asmolov V, Gusev I, Kazanskiy V, Povarov V, Statsura D. New generation first-of-the kind unit – VVER-1200 design features, Nuclear Energy and Technology, cilt Volume 3, no. Issue 4, pp. Pages 260-269, 2017.

[12] IAEA. Status Report-VVER-1200 (V-392), IAEA, Vienna, 2021.

[13] Hafez N, Shahbunder H, Amin E, Elfiki SA, Abdel-Latif A. Study on criticality and reactivity coefficients of VVER-1200 reactor, ScienceDirect, Available: https://www.sciencedirect.com/science/article/pii/S0149197020303401. [Accessed 4 July 2025]., 2021.

[14] Amil M, Jamil M. Fuel Performance Comparison of Uranium Nitride and Uranium Carbide in VVER-1200 using OpenMC, MATEC Web of Conferences," in https://www.researchgate.net/publication/381698162_Fuel_Performance_Comparison_of_Uranium_Nitride_and_Uranium_Carbide_in_VVER-1200_using_OpenMC, 2024.

[15] Kim YK, Sah I, Kim ES. UO_2 Spheres Produced by External Gelation Process, Korean J. Mater.: vol. 30, no. 10, doi: 10.3740/MRSK.2020.30.10.533., Oct. 2020.

[16] Faghihi F, Mirvakili SM, Safaei S, Bagheri S. Neutronics and sub-channel thermal-hydraulics analysis of the Iranian VVER-1000 fuel bundle, Prog. Nucl. Energy, vol. 87, Available: https://www.sciencedirect.com/science/article/pii/S0149197015301001, 2016.

[17] Louis HK. Neutronic Analysis of the VVER-1200 under Normal Operating Conditions, Journal of Nuclear and Particle Physics, cilt Volume: 11(3), pp. Pages: 53-66, 2021.

[18] EE L. Nuclear Power Reactor Safety, USA: John Wiley & Sons, Inc., 1977.

[19] Todreas NE, Kazimi MS. Nuclear Systems, Volume 1: Thermal Hydraulic Fundamentals, Second Edition, CRC Press, Taylor & Francis Group, Boca Raton, London, New York: Pp. [37-40,61,118,198,201,375,548 787-789 and 966], ISBN 978-1-4398-0888-7., 2011.

[20] Vitz E, Moore JW, Shorb J, Prat-Resina X, Wendorff T, Hahn A. Nuclear Power Plants," Chemical Education Digital Library (ChemEd DL). [Çevrimiçi]. Available: https://chem.libretexts.org/Ancillary_Materials/Exemplars_and_Case_Studies/Exemplars/Physics_and_Astronomy/Nuclear_Power_Plants. [Erişildi: 3 July 2025].

[21] Murat O, Sanchez-Espinoza V, Wang S, Stuckert J. Preliminary validation of ASTEC V2.2.b with the QUENCH-20 BWR bundle experiment, Nuclear Engineering and Design, cilt 370, no. ISSN 0029-5493, https://doi.org/10.1016/j.nucengdes.2020.110931., 2020.

[22] Mercan AK, Gabrielli F, Sanchez-Espinoza VH. Validation of Astec2.1 using Quench-12 for VVER-Reactors, Nuclear Engineering and Design, cilt 395, no. 111840, ISSN 0029-5493, 2022.

[23] Lassmann K. TRANSURANUS: a fuel rod analysis code ready for use, Journal of Nuclear Materials, cilt Vol: 188, no. ISSN 0022-3115, pp. Pages 295-302, 1992.